NASA Technical Memorandum 84498

PHENOMENOLOGICAL OPTICAL POTENTIAL ANALYSIS OF PROTON-CARBON ELASTIC SCATTERING AT 200 MeV

H. B. Bidasaria and L. W. Townsend

June 1982

(NASA-TM-84498) PHENOMENOLOGICAL OPTICAL POTENTIAL ANALYSIS OF PROTON-CARBON ELASTIC SCATTERING AT 200 MeV (NASA) 21 p
HC A02/MF A01
CSCL 20H
N82-30066
Unclas
G3/73 28523

National Aeronautics and
Space Administration

Langley Research Center
Hampton, Virginia 23665

Table of Contents

NOMENCLATURE

Symbols:

A_0	harmonic well optical potential parameter (central term), dimensionless
A_1, A_2	harmonic well optical potential parameter (central term), fm^{-2}
B_0	harmonic well optical potential parameter (spin-orbit term), dimensionless
B_1, B_2	harmonic well optical potential parameter (spin-orbit term), fm^{-2}
$\vec{b}$	impact parameter vector, fm
E	projectile kinetic energy in center of mass system, MeV
e	proton charge, esu
$F(\Theta)$	defined in equation (7)
$f(\Theta)$	spin non-flip scattering amplitude, fm
$g(\Theta)$	spin-flip scattering amplitude, fm
$\hbar$	Planck's constant, joule-second
$\vec{J}$	total angular momentum vector, dimensionless
k	center of mass momentum wave number, fm^{-1}
$\vec{L}$	orbital angular momentum vector, dimensionless
M	nucleon mass, kg
$\hat{n}$	unit vector normal to scattering plane, dimensionless
P_L	Legendre polynomial of order L, dimensionless
$P^1{}_L$	associated Legendre function of first kind and order L, dimensionless
$\vec{P}_i$	incident beam polarization vector, dimensionless
$\vec{r}$	relative position vector, fm
$r^{\pm}{}_L$	WKB turning point, fm
r_C	coulomb turning point, fm
$\vec{s}$	spin angular momentum vector, dimensionless

$U^{\pm}$	defined in equation (22)
U_C	defined in equation (21)
V_C	central potential term, MeV
V_S	spin-orbit potential term, MeV
$V^{\pm}_{eff}$	defined in equation (23)
v	relative velocity in center of mass system, m/sec
Z_T	target nuclear charge number, dimensionless
β	defined in equation (11)
Γ	gamma function of complex argument, dimensionless
$\delta_L{}^{\pm}$	defined in equations (16) and (20)
η_L	defined in equation (13)
$\vec{\sigma}$	twice the spin angular momentum, dimensionless
$\sigma(\Theta)$	differential cross section, mb per steradian
Θ	scattering angle, radians
χ	eikonal phase shift, dimensionless

Subscripts:

C	Coulomb
cm	center of mass
c	central
s	spin-orbit
T	target

**ORIGINAL PAGE IS
OF POOR QUALITY**

PHENOMENOLOGICAL OPTICAL POTENTIAL ANALYSIS OF PROTON-CARBON ELASTIC SCATTERING AT 200 MeV

Hari B. Bidasaria
Old Dominion University
Norfolk, Virginia

and

Lawrence W. Townsend
Langley Research Center
Hampton, Virginia

SUMMARY

Differential cross sections for 200 MeV protons elastically scattered from ^{12}C are analyzed utilizing a local, complex, spin-dependent optical potential with a harmonic well radial dependence. Analyses were performed using the WKB and eikonal approximations. For the latter, first-order corrections to the phase shifts were incorporated to account for the spin-orbit contribution. Large disagreement between theory and experiment was observed when the usual Thomas form for the spin-orbit potential was utilized. Substantial improvement was obtained by allowing the parameters in the central and spin-orbit potential terms to vary independently.

ORIGINAL PAGE IS
OF POOR QUALITY

INTRODUCTION

The development of an accurate heavy ion (HZE) transport theory is required to support cosmic ray shielding analyses for future space applications. Transport theory development, in turn, requires a simple, yet accurate, HZE reaction theory as input. For the past several years, such a theory has been under development for incident projectile energies above several hundred MeV/amu (refs. 1-7). At present, no satisfactory theory exists for energies below (approximately) 200 MeV/amu where the eikonal (high energy) approximation appears to become inadequate (refs. 3 and 6). At lower incident kinetic energies, contributions from low order partial waves (orbital angular momentum states) increase appreciably. In addition, the incident ion's trajectory deviates significantly from its initial straight line path such that the eikonal approximation may no longer yield accurate predictions. At these lower energies, a better approximation is the Wentzel-Kramers-Brillouin (WKB) method (ref. 8). This work describes our initial investigation into utilizing this approximation method to analyze elastic scattering. Proton-carbon scattering was chosen for analytic convenience due to its simplicity (elementary rather than composite projectile) and because it is the subject of much current theoretical and experimental interest (refs. 9-11). Additionally, a harmonic well potential parameterization rather than the usual Woods-Saxon form (refs. 9 and 10) was chosen since it more accurately represents the actual carbon nuclear distribution (refs. 7 and 12) and should therefore yield agreement with experimental data for fewer free parameters than the 24 required by the double-Woods-Saxon potential analysis of reference 9.

ANALYTIC METHODS
Optical Potential Parameterization

The optical potential chosen for this analysis consisted of a central, V_c, and spin-orbit, V_s, contribution (ref. 8)

$$V(\vec{r}) = V_c(\vec{r}) + \vec{\sigma} \cdot \vec{L}\, V_s(\vec{r}) \tag{1}$$

where $\vec{\sigma}$ is twice the spin angular momentum, $\vec{s}$, and $\vec{L}$ the orbital angular momentum vector for the incident proton. The scalar product $\vec{\sigma} \cdot \vec{L}$ is

$$\vec{\sigma} \cdot \vec{L} = \begin{cases} L & \text{, parallel} \\ -(L + 1) & \text{, antiparallel} \end{cases} \tag{2}$$

where parallel/antiparallel refers to the relative orientation of $\vec{\sigma}$ with respect to the total angular momentum vector

$$\vec{J} = \vec{L} + (1/2)\,\vec{\sigma} \ . \tag{3}$$

From reference 13, the spin-independent central potential for p - ^{12}C scattering, using a harmonic well charge distribution for ^{12}C, is of the form

$$V_c(\vec{r}) = A_0 (1 + A_1 r^2) \exp(-A_2 r^2) \tag{4}$$

where A_0 is complex and A_1 and A_2 are real. The usual Thomas-Fermi form for the spin-orbit contribution is (ref. 11)

$$V_s(\vec{r}) = \frac{1}{r} \frac{d}{dr} V_c(\vec{r}) \tag{5}$$

which can also be parameterized as

$$V_s(\vec{r}) = B_0 (1 + B_1 r^2) \exp(-B_2 r^2) \tag{6}$$

with B_0 complex and B_1 and B_2 real. Using equations (4) and (5) it can be shown that the B_i $(i = 0 - 2)$ are functions of the A_i and that $B_2 = A_2$. In this work, these parameters are treated as completely free. Hence, we find that the restrictions imposed on the B_i by equation (5) do not hold and in particular, $B_2 \neq A_2$ (see RESULTS).

Scattering Formalism

From reference 8, the scattering amplitude is

$$F\ (\Theta) = f\ (\Theta) + \vec{\sigma} \cdot \hat{n}\ g\ (\Theta) \tag{7}$$

where $\hat{n}$ is the unit vector normal to the scattering plane and

$$\begin{aligned} f\ (\Theta) = {} & f_C\ (\Theta) + (2ik)^{-1} \sum_{L=0}^{\infty} \exp\ (2i\eta_L) \\ & \times \Big\{ (L + 1)\ [\exp\ (2i\delta_L^{+}) - 1] \\ & + L\ [\exp\ (2i\delta_L^{-}) - 1] \Big\}\ P_L\ (\cos\ \Theta) \end{aligned} \tag{8}$$

$$g\ (\Theta) = (2k)^{-1} \sum_{L=1}^{\infty} [\exp\ (2i\delta_L^{+}) - \exp\ (2i\delta_L^{-})]\ P_L^1\ (\cos\ \Theta) \tag{9}$$

where $f_C(\Theta)$, the coulomb scattering amplitude is

$$f_C\ (\Theta) = -[\beta/2k\ \sin^2(\Theta/2)]\ \exp\ [2i\eta_0 - i\beta\ \ln\ \sin^2(\Theta/2)]\ . \tag{10}$$

In equations (8) through (10) above, k is the center of mass wave number, the δ_L are the phase shifts (to be determined in the following sections), the $P_L(\cos\ \Theta)$ are Legendre polynomials, and $P_L^1(\cos\ \Theta)$ are associated Legendre functions of the first kind (see ref. 14). Additionally, for the coulomb contribution, we use

$$\beta = Z_T e^2/hv \tag{11}$$

$$\eta_0 = \mathrm{Arg}\ \Gamma\ (1 + i\beta) \tag{12}$$

and

$$\eta_L = \eta_{L-1} + \tan^{-1}\ (\beta/L) \tag{13}$$

where v is the relativistic relative velocity between the projectile and target.

The elastic differential cross section is then given by

$$\frac{d\sigma}{d\Omega} = \sigma\ (\Theta) = |\ F\ (\Theta)\ |^2 \tag{14}$$

which, from equations (7) through (10) yields

$$\sigma (\theta) = | f (\theta) |^2 + | g (\theta) |^2 + 2 \text{ Re } (f^* g) \langle \hat{n} \cdot \vec{P}_i \rangle \qquad (15)$$

where $\vec{P}_i$ is the polorization of the incident beam.

Eikonal Phase Shifts

In terms of the eikonal phases, χ, the partial wave phase shifts, with first order corrections (ref. 11) to account for the spin-orbit contribution, are

$$\delta_L^{\pm} = (1/2) \{\chi_c (\vec{b}) \pm (kb \mp 1/2) \chi_s (\vec{b})\} \tag{16}$$

where

$$kb = L + 1/2 \tag{17}$$

and

$$\chi_c (\vec{b}) = -(m/k) \int_{-\infty}^{\infty} V_c (\vec{r}) \, dz \tag{18}$$

$$\chi_s (\vec{b}) = -(m/k) \int_{-\infty}^{\infty} V_s (\vec{r}) \, dz \; . \tag{19}$$

WKB Phase Shifts

To first order, the WKB phase shifts for outgoing scattered waves are given by (ref. 15).

$$\delta_L^{\pm} = \int_{r_L^{\pm}}^{\infty} k\,[1 - U^{\pm}(r,L)]^{1/2}\,dr - \int_{r_C}^{\infty} k\,[1 - U_c\,(r,L)]^{1/2}\,dr \tag{20}$$

where

$$U_C\,(r,L) = \frac{L(L+1)}{2mr^2 E} + \frac{Z_T e^2}{Er} \tag{21}$$

and

$$U^{\pm}\,(r,L) = V_{eff}^{\pm}/E \tag{22}$$

with

$$V_{eff}^{\pm} = \frac{L(L+1)}{2mr^2} + \left\{ \begin{array}{l} V_c + LV_s \\ V_c - (L+1)\,V_s \end{array} \right\} + \frac{Z_T e^2}{r}\,. \tag{23}$$

In the above expressions, E is the projectile kinetic energy in the center of mass system. The complex turning points $r_L^{\pm}$ and r_C are those values of r for which

$$1 - U^{\pm}\,(r,L) = 0 \tag{24}$$

and

$$1 - U_C\,(r,L) = 0 \tag{25}$$

respectively. These were located using a computer search routine based upon the Newton-Raphson method in the complex plane (ref. 16). The integrals for the complex phase shifts in equation (20) were then evaluated numerically.

RESULTS

Figure 1 displays theoretical cross sections obtained using equation (15) with eikonal phase shifts obtained from equation (16). For comparison, the experimental results from reference 9 are also displayed. The polarization of the incident beam was approximately 70 percent (ref. 9). The optical potential parameter values utilized for the analysis, listed in Table I, were obtained using a gradient-search least-squares fit to minimize the chi-squared deviation between the theoretical predictions and experimental results (ref. 17). As displayed in Figure 1, the agreement between theory and experiment is excellent except for small angles ($\Theta_{cm} < 10^\circ$). This disagreement is not unexpected when using an eikonal formalism (ref. 18). Table II displays the calculated parameters for the Thomas-Fermi spin-orbit form from equation (5). Comparing Tables I and II shows the calculated parameter values to be quite different than the parameter values obtained with the computer search.

Figures 2 and 3 display results utilizing the WKB approximation. Complex turning points obtained from equation (24) are shown in Figure 2. For these calculations the potential parameters used in equations (4) and (5) are those listed in Table I. Note that all turning points lie on or near the real axis. Figure 3 displays the cross sections obtained using WKB phase shifts. Improved agreement between theory and experiment is noted for small angles. There is, however, significant disagreement for large angles ($\Theta_{cm} > 55^\circ$). This is likely due to the use of the potential parameters obtained from the eikonal phase shift search. Improvement should be obtained when the parameter search using WKB phase shifts is conducted, since the previously mentioned eikonal shortcoming for small angles should be corrected. A parameter search utilizing WKB phase shifts will, however, be very time-consuming since any change in a parameter requires that all turning points and phase shifts be re-determined. Upon completing the parameter search with the WKB method, the conclusion concerning the use of the Thomas-Fermi form for the spin-orbit contribution should be rechecked since the previous conclusion may no longer be valid.

ORIGINAL PAGE IS
OF POOR QUALITY

CONCLUDING REMARKS

This work has demonstrated that reasonably good agreement between theory and experiment can be obtained with only 8 parameters in the nuclear potential. The use of potential parameters, obtained from an eikonal formalism, for a WKB analysis, is probably not adequte but may serve as a useful starting point for a WKB parameter search. Other improvements to the theory could be made by discarding the point-charge Coulomb potential in favor of a more realistic extended charge distribution. Coulomb spin-orbit effects and Pauli blocking effects should also be included. The latter, however, will increase the number of free parameters from 8 to 16.

REFERENCES

1. Wilson, J. W.: Multiple Scattering of Heavy Ions, Glauber Theory, and Optical Model. Physics Letters, vol. B52, no. 2, September 1974, pp. 149-152.
2. Wilson, J. W.: Composite Particle Reaction Theory. Ph.D. dissertation, The College of William and Mary in Virginia, June 1975.
3. Wilson, J. W.; and Costner, C. M.: Nucleon and Heavy-Ion Total and Absorption Cross Section for Selected Nuclei. NASA TN D-8107, 1975.
4. Wilson, J. W.; and Costner, C. M.: High-Energy Heavy Ion Absorption Cross Section. NASA TM X-73929, 1976.
5. Townsend, L. W.: Optical Model Abrasion Cross Sections for High-Energy Heavy Ions. NASA TP-1893, 1981.
6. Wilson, J. W.; and Townsend, L. W.: An Optical Model for Composite Nuclear Scattering. Canadian Journal of Physics, vol. 59, no. 11, November 1981, pp. 1569-1576.
7. Townsend, L. W.: Harmonic Well Matter Densities and Pauli Correlation Effects in Heavy-Ion Collisions. NASA TP-2003, 1982.
8. Joachain, Charles J.: Quantum Collision Theory. American Elsevier Publishing Company, Inc., 1975.
9. Meyer, H. O.; Schwandt, P.; Moake, G. L.; and Singh, P. P.: Elastic Scattering of 200 MeV Polarized Protons from ^{12,13}C and the Optical Potential. Physical Review C, vol. 23, no. 2, February 1981, pp. 616-622.
10. Blanpied, G. S.; Hoffmann, G. W.; Barlett, M. L.; McGill, J. A.; Greene, S. J.; Ray, L.; Van Dyck, O. B.; Amann, J.; and Thiessen, H. A.: Large Angle Scattering of 0.8 GeV Protons from ^{12}C. Physical Review C, vol. 23, no. 6, June 1981, pp. 2599-2605.
11. Waxman, D.; Wilkin, C.; Germond, J. F.; and Lombard, R. J.: Eikonal Corrections for Spin-Orbit Potentials. Physical Review C, vol. 24, no. 2, August 1981, pp. 578-587.
12. De Jager, C. W.; De Vries, H.; and De Vries, C.: Nuclear Charge and Magnetization-Density-Distribution Parameters from Elastic Electron Scattering. At. Data & Nucl. Data Tables, vol. 14, no. 5/6, Nov/Dec 1974, pp. 479-508.
13. Bidasaria, H. B.; and Townsend, L. W.: Analytic Optical Potentials for Nucleon-Nucleus and Nucleus-Nucleus Collisions Involving Light and Medium Nuclei. NASA TM-83224, 1982.
14. Gradshteyn, I. S.; and Ryzhik, I. M.: Table of Integrals, Series, and Products. Academic Press, 1965.

ORIGINAL PAGE IS
OF POOR QUALITY

15. Chan, C. K.; Suebka, P.; and Lu, P: Higher-Order WKB Phase Shifts for the Heavy-Ion Optical Potential. Physical Review C, vol. 24, no. 5, November 1981, pp. 2035-2037.

16. James, M. L.; Smith, G. M.; and Wolford, J. C.: Applied Numerical Methods for Digital Computation with Fortran and CSMP, Second Edition. Harper & Row, 1977.

17. Bevington, P. R.: Data Reduction and Error Analysis for the Physical Sciences. McGraw-Hill Book Co., 1969.

18. Glauber, R.: Asymptotic Diffraction Theory. Proceedings of the Fifth High Energy Heavy Ion Study, Berkeley, CA, May 18-22, 1981, Lawrence Berkeley Laboratory Report No. LBL-12652, p. 396.

Table I. - Optical Potential Parameters from the Eikonal Formalism Search

$A_0 = -4.95 - i\ 48.01$ MeV

$A_1 = 0.380\ \mathrm{fm}^{-2}$

$A_2 = 0.495\ \mathrm{fm}^{-2}$

$B_0 = 8.52 + i\ 1.81$ MeV

$B_1 = 0.431\ \mathrm{fm}^{-2}n$

$B_2 = 0.688\ \mathrm{fm}^{-2}$

Table II. - Calculated Thomas-Fermi Spin-Orbit Parameters

$B_0 = 1.14 + i\ 11.04$ MeV

$B_1 = 1.636\ \text{fm}^{-2}$

$B_2 = 0.495\ \text{fm}^{-2}$

ORIGINAL PAGE IS
OF POOR QUALITY

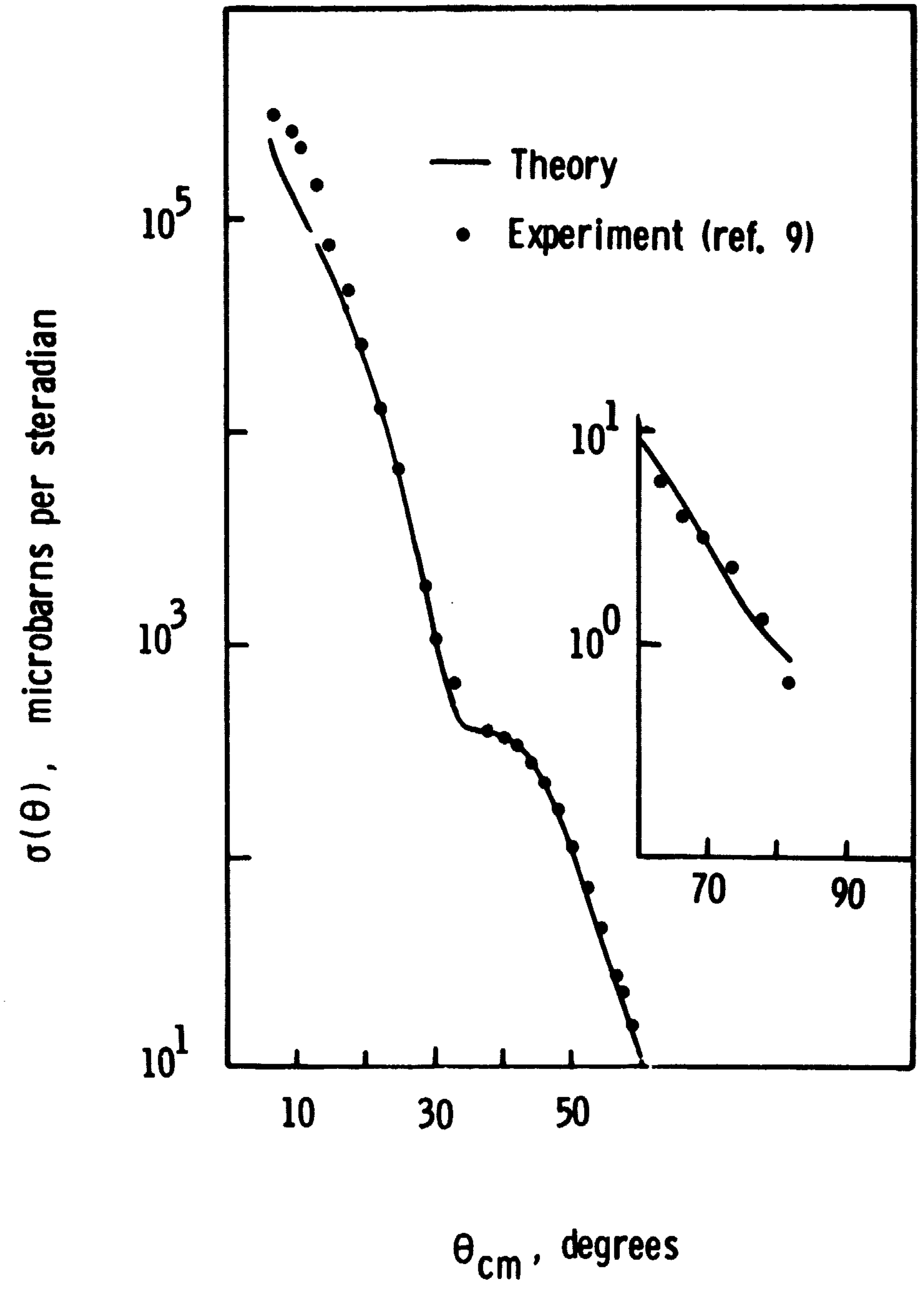

Figure 1. 200 MeV proton-carbon elastic scattering differential cross sections. The theoretical curve was obtained using eikonal phase shifts.

ORIGINAL PAGE IS
OF POOR QUALITY

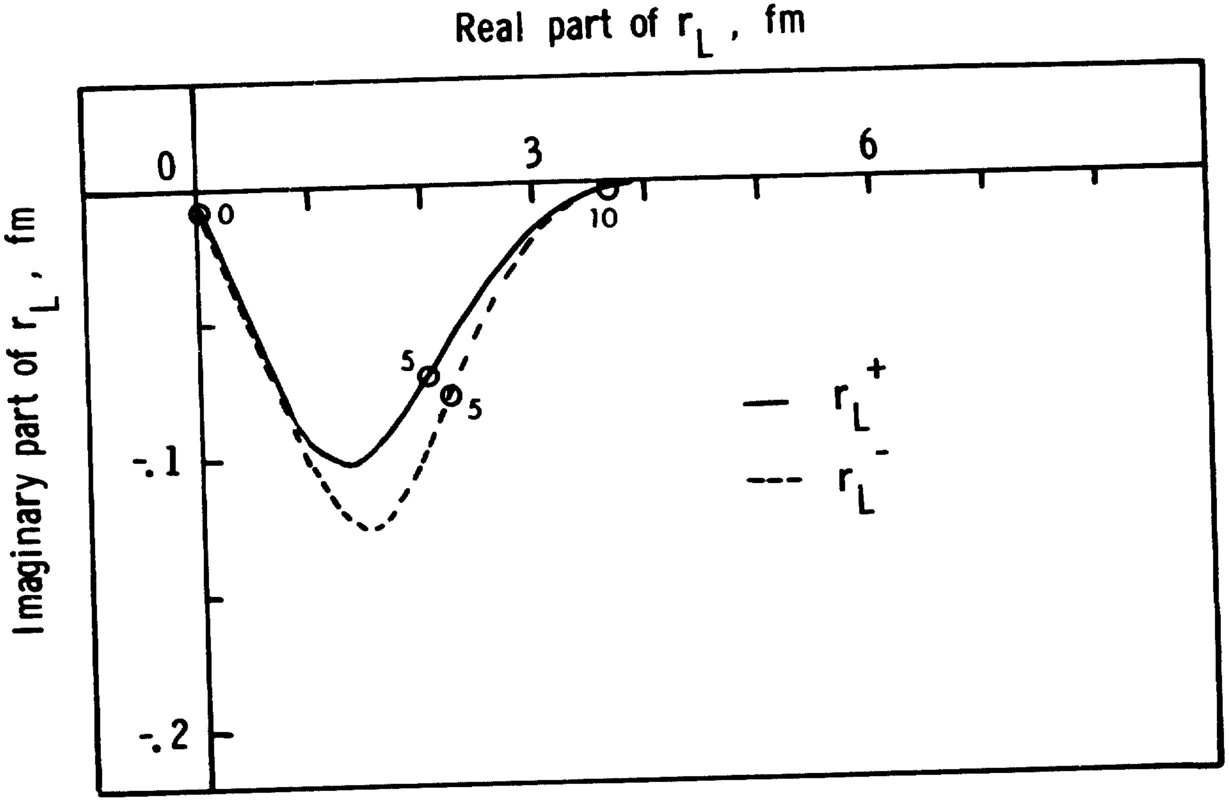

Figure 2. Complex WKB turning points as a function of the orbital angular momentum quantum number for 200 MeV proton-carbon scattering.

ORIGINAL PAGE IS
OF POOR QUALITY

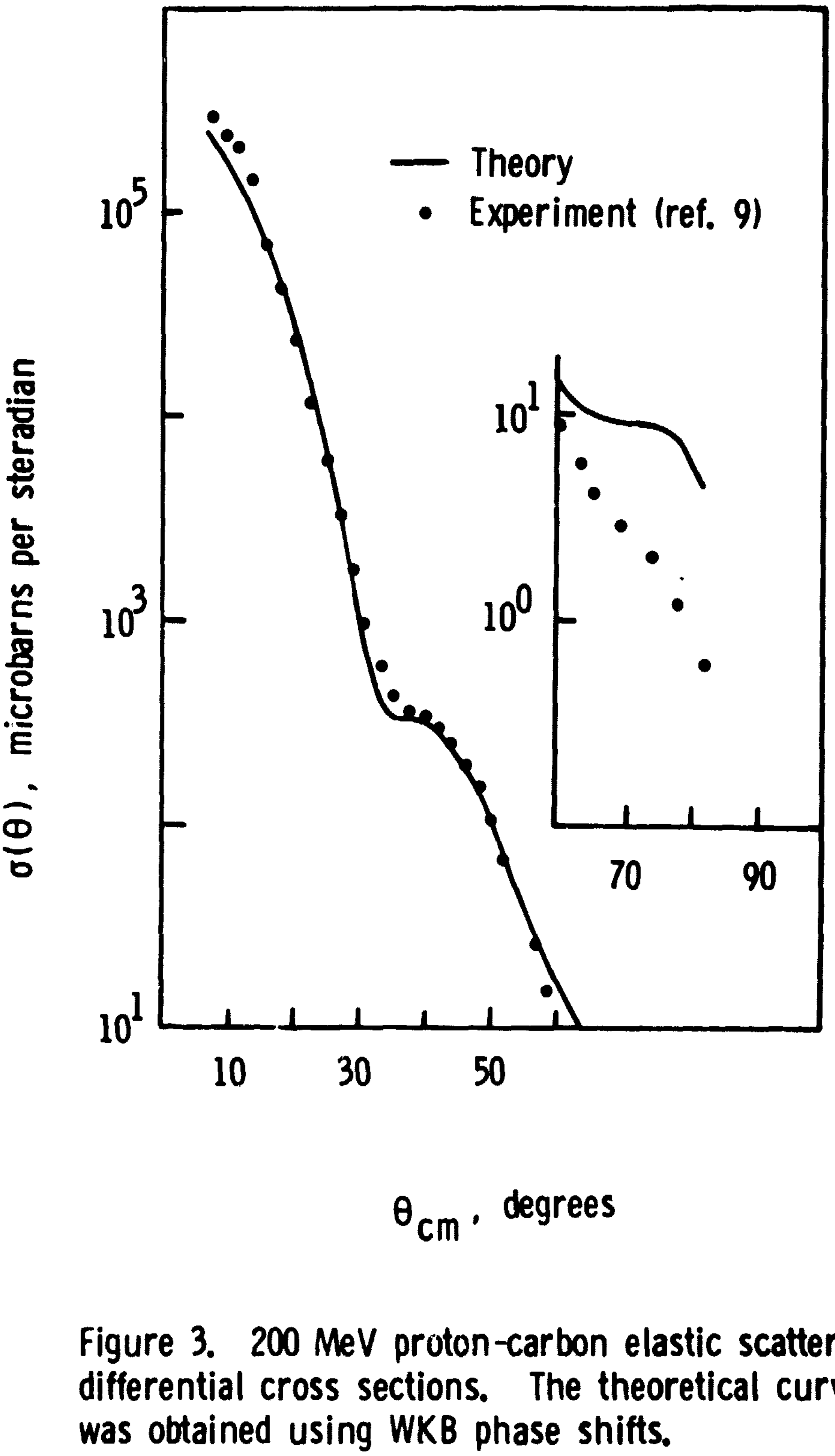

Figure 3. 200 MeV proton-carbon elastic scattering differential cross sections. The theoretical curve was obtained using WKB phase shifts.